

Magnetic properties of $S = 5/2$ anisotropic triangular chain $\text{Bi}_3\text{FeMo}_2\text{O}_{12}$

K. Boya,¹ K. Nam,² A. K. Manna,³ J. Kang,² C. Lyi,² A. Jain,^{4,5} S. M. Yusuf,^{4,5} P. Khuntia,⁶ B. Sana,⁶ V. Kumar,⁷ A. V. Mahajan,⁷ Deepak. R. Patil,² Kee Hoon Kim,² S. K. Panda,^{8,*} and B. Koteswararao^{1,†}

¹*Department of Physics, Indian Institute of Technology Tirupati, Tirupati 517 506, India*

²*Department of Physics and Astronomy and Institute of Applied Physics, Seoul National University, Seoul 151-747, Republic of Korea*

³*Department of Chemistry, Indian Institute of Technology Tirupati, Tirupati 517 506, India*

⁴*Solid State Physics Division, Bhabha Atomic Research Centre, Mumbai 400085, India*

⁵*Homi Bhabha National Institute, Anushaktinagar, Mumbai 400094, India*

⁶*Department of Physics, Indian Institute of Technology Madras, Chennai 600 036, India*

⁷*Department of Physics, Indian Institute of Technology Bombay, Mumbai 400 076, India*

⁸*Department of Physics, Bennett University, Greater Noida 201310, Uttar Pradesh, India*

(Dated: October 26, 2021)

Abstract

Competing magnetic interactions in low-dimensional quantum magnets can lead to the exotic ground state with fractionalized excitations. Herein, we present our results on an $S = 5/2$ quasi-one-dimensional spin system $\text{Bi}_3\text{FeMo}_2\text{O}_{12}$. The structure of $\text{Bi}_3\text{FeMo}_2\text{O}_{12}$ consists of very well separated, infinite zig-zag $S = 5/2$ spin chains. The observation of a broad maximum around 10 K in the magnetic susceptibility $\chi(T)$ suggesting the presence of short-range spin correlations. $\chi(T)$ data do not fit to $S = 5/2$ uniform spin chain model due to the presence of 2^{nd} nearest-neighbor coupling (J_2) along with the 1^{st} nearest-neighbor coupling (J_1) of the zig-zag chain. The electronic structure calculations infer that the value of J_1 is comparable with J_2 ($J_2/J_1 \approx 1.1$) with a negligible inter-chain interaction ($J'/J \approx 0.01$) implying that $\text{Bi}_3\text{FeMo}_2\text{O}_{12}$ is a highly frustrated triangular chain system. The absence of magnetic long-range ordering down to 0.2 K is seen in the heat capacity data, despite a relatively large antiferromagnetic Curie-Weiss temperature $\theta_{CW} \approx -40$ K. The magnetic heat capacity follows nearly a linear behavior at low temperatures indicating that the $S = 5/2$ anisotropic triangular chain exhibits the gapless excitations.

PACS numbers:

I. INTRODUCTION

Investigating the exotic magnetic properties of low-dimensional and geometrically frustrated spin systems is one of the active research fields in modern condensed matter physics [1–4]. Mermin-Wagner theorem states that the system with dimensionality $d \leq 2$ and finite range interactions preserve continuous symmetry [5]. The quantum fluctuations, in general, originated from quantum effects, are intrinsic and significant in low-dimensional magnetic systems (LDMS). These are further prominent for low spin ($S = 1/2$) magnetic materials. The physics of $S = 1/2$ LDMS is quite rich, and they offer a viable ground for the experimental realization of correlated quantum states with exotic fractional excitations [1, 2]. The algebraic spin-spin correlation decay in $S = 1/2$ uniform spin chain systems suggests that the ground state is gapless [6–8]. Further, the introduction of geometric frustration through the presence of 2^{nd} nearest neighbor (NN) interaction (J_2) along with that of 1^{st} NN interaction (J_1) to the $S = 1/2$ uniform spin chain leads to a gapped excitation spectrum in the ground state as per the exactly solvable Majumdar-Ghosh (MG) chain model [9]. The MG chain model states that $J_2/J_1 = 0.5$ opens a spin-gap and forms a singlet ground state [10].

On the other hand, the LDMS with large spin (i.e., $S = 5/2$) has not been studied extensively as the quantum effects are not prominent in these materials. A few examples with $S = 5/2$ systems are $\text{SrMn}_2\text{V}_2\text{O}_8$ [11], $\text{SrMn}(\text{VO}_4)(\text{OH})$ [12], $\text{Ba}_3\text{Fe}_2\text{Ge}_4\text{O}_{14}$ [13], and $\text{Bi}_2\text{Fe}(\text{SeO}_3)\text{OCl}_3$ [14]. For example, the Mn-based linear chain system $\text{SrMn}_2\text{V}_2\text{O}_8$ exhibits a broad maximum (T^{max}) in the susceptibility data $\chi(T)$ around 200 K. However, due to the presence inter-chain couplings ($J'/J_1 \geq 0.6$), this material shows a magnetic long-range order (LRO) at 45 K. The Fe-based zig-zag chain $\text{Bi}_2\text{Fe}(\text{SeO}_3)\text{OCl}_3$ system shows T^{max} around 130 K in the $\chi(T)$ data and LRO at 13 K, even in the presence of magnetic frustration with $J_2/J_1 \approx 0.2$. All these $S = 5/2$ spin systems undergo LRO at finite temperature due to the inter-chain coupling and insufficient magnetic frustration. It is pertinent to ask whether a correlated dynamic ground state is realizable or not in low dimensional systems with large spin. In this context, exploring novel low dimensional spin systems with large spin $S = 5/2$ promising to host quantum spin liquid with exotic fractional excitations set an attractive setting.

In this paper, we report the magnetic properties and electronic structure calculations on $\text{Bi}_3\text{FeMo}_2\text{O}_{12}$ [15]. This material comprises the very well separated $S = 5/2$ zig-zag chains passing along the c -axis. The magnetic moments ($S = 5/2$) interact antiferromagnetically with Curie-Weiss temperature $\theta_{CW} \approx -40$ K. No magnetic LRO or spin freezing is observed down to 0.2 K. From the electronic structure calculations, the estimated ratio

*Electronic address: swarup.panda@bennett.edu.in

†Electronic address: koteswararao@iittp.ac.in

of 2^{nd} NN and 1^{st} NN couplings between Fe atoms is close to 1.1, and negligible inter-chain coupling ($J'/J_1 \approx 0.01$), which suggests that the $\text{Bi}_3\text{FeMo}_2\text{O}_{12}$ is a unique material with very well separated $S = 5/2$ triangular chains with a small anisotropy. Interestingly, heat capacity shows a nearly linear behavior with a finite value of the linear coefficient, suggesting the gapless excitations in the $S = 5/2$ triangular chains, unlike the $S = 1/2$ triangular chains that host a spin-gap ground state [16].

II. EXPERIMENTAL DETAILS

The polycrystalline samples of $\text{Bi}_3\text{FeMo}_2\text{O}_{12}$ and the non-magnetic analog $\text{Bi}_3\text{GaMo}_2\text{O}_{12}$ were synthesized by solid-state reaction method using the respective chemicals of Bi_2O_3 , Fe_2O_3 , Ga_2O_3 , and MoO_3 . These chemicals are mixed in stoichiometric ratio and thoroughly grounded in agate mortar and pestle. The pellets were made using the hydraulic press and heated at different temperatures from 400°C to 800°C . Finally, the sample was fired at 800°C for 72 hours with a few intermediate grindings to obtain the single phase of the samples $\text{Bi}_3\text{FeMo}_2\text{O}_{12}$. Neutron powder diffraction (NPD) experiments were performed using the neutron powder diffractometer PD-I ($\lambda = 1.094 \text{ \AA}$) with three linear position-sensitive detectors at Dhruva reactor, Bhabha Atomic Research Center, India. Magnetization (M), and heat capacity (C_p) measurements were performed on the polycrystalline sample pellets using the Physical Properties Measurement System (PPMS) with the corresponding attachments of Vibration Sample Magnetometer (VSM) and heat-capacity measurement option, respectively, in the temperature range from 2 K to 300 K and in the magnetic fields up to 160 kOe. Low-temperature heat capacity data was measured using a dilution fridge on a flat pellet of $\text{Bi}_3\text{FeMo}_2\text{O}_{12}$.

III. RESULTS

A. Structural details

$\text{Bi}_3\text{FeMo}_2\text{O}_{12}$ crystallizes in a monoclinic structure with a space group $C2/c$ and holds the Scheelite-type structure with ABO_4 family [15]. The Bi atoms are located at the A-site, while B-site is occupied by Fe and Mo atoms in $\text{Bi}_3\text{FeMo}_2\text{O}_{12}$ structure. Interestingly, the Fe and Mo atoms are ordered at the B-site. The unit cell consists of FeO_4 , MoO_4 tetrahedral, and BiO_6 polyhedral units (see Fig. 1(a)). The obtained lattice parameters from the Rietveld refinement of XRD pattern are $a = 16.91 \text{ \AA}$, $b = 11.65 \text{ \AA}$, and $c = 5.25 \text{ \AA}$, $\alpha = \gamma = 90^\circ$, $\beta = 107.1^\circ$. The Fe^{3+} ($S = 5/2$) ions form an infinite zig-zag chain running along the c -axis, as shown in Fig. 1(b). The 1^{st} NN distance of Fe-Fe is 3.79 \AA with a possible exchange path of Fe-O1-O1-Fe. The 2^{nd} NN distance of Fe-Fe is 5.25 \AA , and its possible exchange path could be through Fe-O2-O2-Fe interactions. The bond lengths

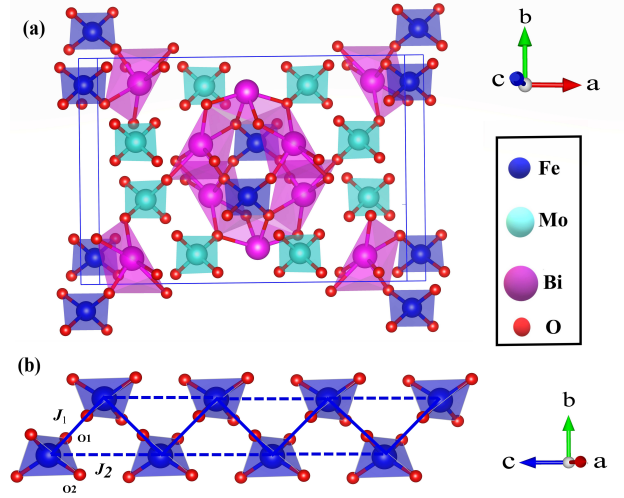


Figure 1: (Color online) (a) Unit cell of $\text{Bi}_3\text{FeMo}_2\text{O}_{12}$ [15]. (b) FeO_4 tetrahedral units form the zig-zag chain running along c -axis. The 1^{st} NN Fe-Fe distance is 3.8 \AA (with exchange coupling J_1) and 2^{nd} NN Fe-Fe distance is 5.3 \AA (with exchange coupling J_2).

and bond angles are shown in the table I. These chains are very well separated by a relatively large distance of 8.64 \AA , suggesting that the compound might have nearly isolated $S = 5/2$ zig-zag spin chains.

B. Neutron diffraction measurements

The data were recorded at different temperatures from 6 K to 50 K. Rietveld refinement of NPD data was performed using the FullProf Suite software package as shown in Fig. 2(a), (b), and (c). The observed neutron diffraction pattern could be fitted by considering only the nuclear phase. We have subtracted the intensities of 50 K from 6 K data, i.e., $I(50 \text{ K}) - I(6 \text{ K})$. We do not see any signs of new Bragg intensities or diffuse background patterns from the subtracted data as shown in Fig. 2(d). We have also compared the difference plot of $I(50 \text{ K}) - I(6 \text{ K})$ with the difference plot of $I(50 \text{ K}) - I(20 \text{ K})$, and there is no difference seen between these two plots. Neither additional magnetic Bragg peaks nor an enhancement in the intensity of the fundamental nuclear Bragg peaks has been observed down to 6 K (see Fig. 2(d)), indicating the absence of magnetic long-range order and rule out the presence of a phase transition at 11 K as was reported in reference [17].

C. Magnetization measurements

Temperature-dependent magnetic susceptibility $\chi(T)$ measurements were performed on the polycrystalline sample $\text{Bi}_3\text{FeMo}_2\text{O}_{12}$ in the T range from 2 - 300 K in $H = 10 \text{ kOe}$ (see Fig. 3(a)). The fit of the $\chi(T)$ data to Curie-Weiss law yields the temperature-independent susceptibility $\chi_0 \approx -2.0 \times 10^{-4} \text{ cm}^3/\text{mol}$, Curie-Weiss temperature $\theta_{CW} \approx -40 \text{ K}$, and Curie constant $C \approx 4.3 \text{ cm}^3 \text{ K/mol}$. Diamagnetic susceptibility is estimated to be $\chi_{dia} \approx 2.4 \times 10^{-4} \text{ cm}^3/\text{mol}$ from the individual ions in the formula $\text{Bi}_3\text{FeMo}_2\text{O}_{12}$. After the subtraction of

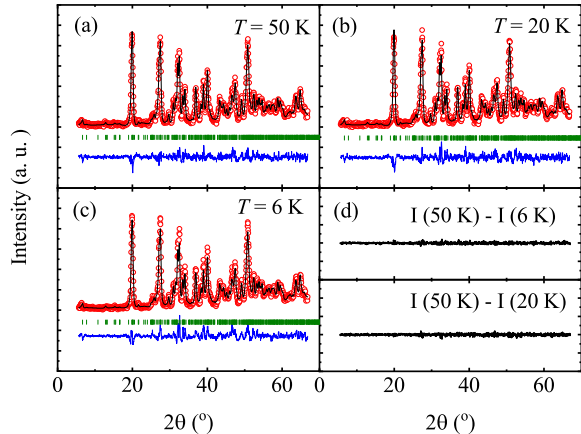


Figure 2: (Color online) Rietveld refinement of Neutron diffraction (ND) data measured at different temperatures 50 K, 20 K, and 6 K are shown in (a), (b), and (c), respectively. Red circles represent the measured data (I_{obs}), the black line represents the calculated diffraction pattern (I_{cal}), the blue line represents the difference ($I_{obs} - I_{cal}$), and the green vertical lines represent the Bragg positions. (d) The ND intensities of 6 K and 20 K after subtracting the ND intensities at 50 K.

χ_{dia} from the obtained value of χ_0 , the calculated Van Vleck susceptibility is $\chi_{vv} \approx 4.2 \times 10^{-5} \text{cm}^3/\text{mol}$. From the value of C , the effective magnetic moment of Fe^{3+} is calculated to be $5.90 \mu_B$ ($= \sqrt{8C} \mu_B$), well consistent with the expected value of $5.91 \mu_B$ for $S = 5/2$. The absence of splitting in zero-field-cooled (ZFC) and field-cooled (FC) susceptibility rules out the spin-glass transition in this compound, as shown in the inset of Fig. 3(a). Fig. 3(b) represents the magnetization isotherm at 2 K was measured up to 160 kOe. The $M(H)$ follows linear behavior, indicating the absence of ferromagnetic components in the samples. $M(H)$ data do not saturate up to 160 kOe field. The large magnetic field is required to reach saturated magnetization $M_{sat} = gS = 5\mu_B$ for $S = 5/2$ magnetic moments.

At low- T , $\chi(T)$ shows a broad maximum around $T^{max} \approx 10$ K, indicating the presence of short-range correlations [6, 18–20]. We tried to analyze $\chi(T)$ with $S = 5/2$ uniform spin chain model by Bonner and Fisher (BF) [21, 22] and found that this model could not reproduce our experimental data. According to the $S = 5/2$ uniform spin chain, the broad maximum would appear at $k_B T^{max}/J = 10.6$ [23]. From our experimental observation of T^{max} position, the J/k_B value expected to be about -1 K [23]. We have then compared the experimental data with the $S = 5/2$ uniform chain model with $J/k_B \approx -1$ K. As shown in the inset of Fig. 3(b), the experimental value of magnetic susceptibility is much smaller than the simulated data, suggesting the presence of significant additional antiferromagnetic exchange couplings. From this analysis, we anticipated the presence of a significant value of 2^{nd} NN coupling along with 1^{st} NN

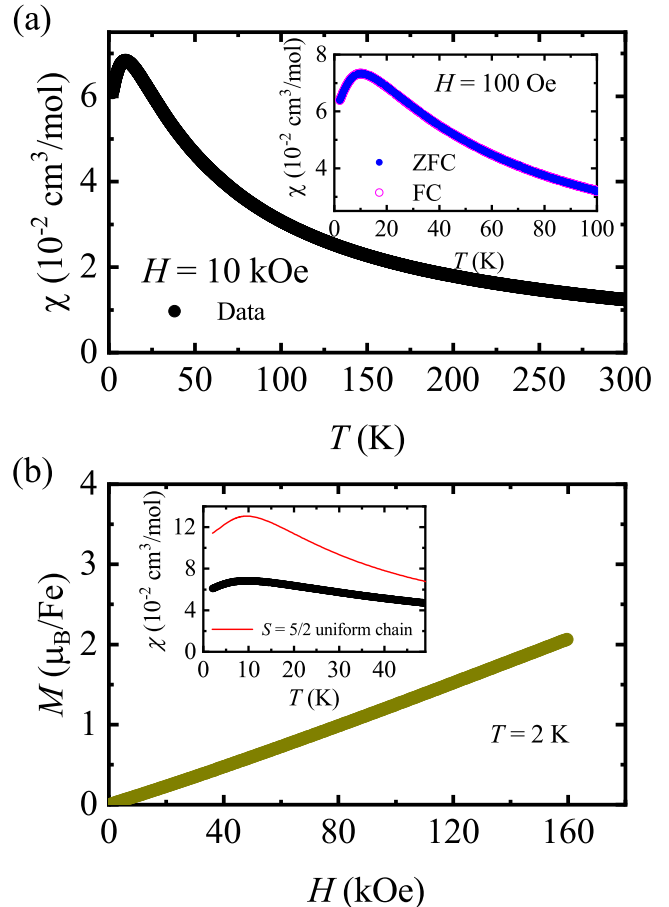


Figure 3: (Color online) (a) Temperature-dependent magnetic susceptibility from 2 K to 300 K. The inset of figure (a) shows the ZFC and FC magnetic susceptibility data under 100 Oe field. (b) Magnetic isotherm measured at $T = 2$ K with variation of field 160 kOe. The inset shows the comparison of experimental data with $S = 5/2$ uniform spin chain simulation for $J/k_B \approx -1$ K.

coupling qualitatively. This is further quantitatively confirmed from the first-principle density functional theory (DFT) electronic structure calculations discussed later in the paper. The presence of 2^{nd} NN exchange coupling accounts for the large magnetic frustration in this material since J_1 , and J_2 form a triangular network (see Fig. 1(b)).

D. Heat capacity measurements

The heat capacity $C_p(T)$ data of $\text{Bi}_3\text{FeMo}_2\text{O}_{12}$ and $\text{Bi}_3\text{GaMo}_2\text{O}_{12}$ were investigated in zero field (see Fig. 4). At low- T , there is a large difference seen between the C_p of $\text{Bi}_3\text{FeMo}_2\text{O}_{12}$ and $\text{Bi}_3\text{GaMo}_2\text{O}_{12}$ indicating the dominance of magnetic contribution. Interestingly, no sharp peak is observed down to 0.2 K in the $C_p(T)$ data of $\text{Bi}_3\text{FeMo}_2\text{O}_{12}$, suggesting the absence of magnetic LRO. The frustration parameter $f = |\theta_{CW}|/T_N$ value

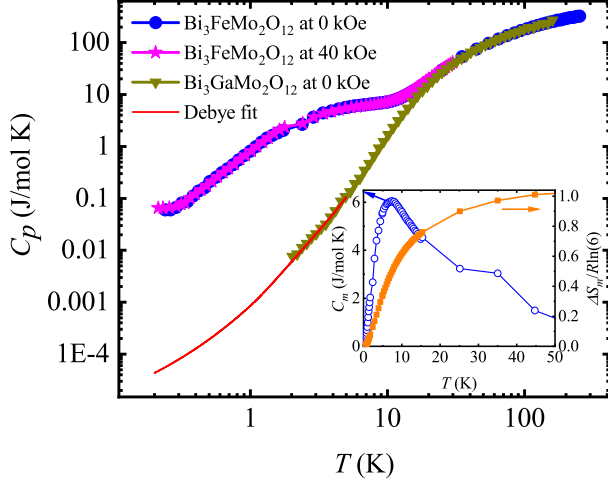


Figure 4: (Color online) Temperature-dependent heat capacity $C_p(T)$ data of $\text{Bi}_3\text{FeMo}_2\text{O}_{12}$ and $\text{Bi}_3\text{GaMo}_2\text{O}_{12}$ with lattice part of the heat capacity data (red) extracted from Debye fit. The observed lattice contribution of the non-magnetic analog is extremely small at low temperatures, compared to the heat capacity of $\text{Bi}_3\text{FeMo}_2\text{O}_{12}$. Inset shows the magnetic heat capacity C_m (left) and normalized magnetic entropy ΔS_m (right) versus T .

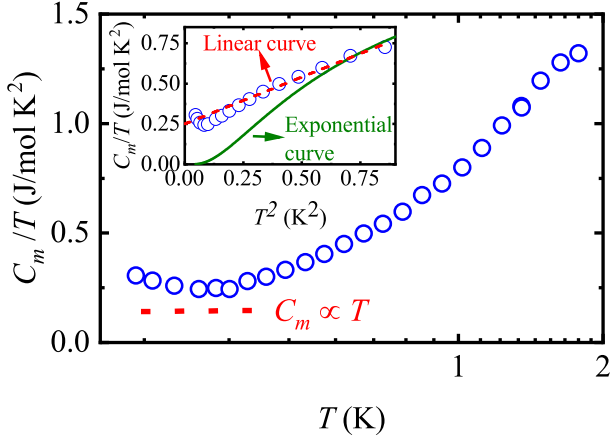


Figure 5: (Color online) C_m/T vs. T plot. Inset shows C_m/T vs. T^2 with the comparison of linear and exponential curves.

is greater than 200, indicating the presence of strong spin frustration. To extract the magnetic contribution $C_m(T)$, we have used the C_p data of its non-magnetic analog $\text{Bi}_3\text{GaMo}_2\text{O}_{12}$ [24]. C_p data of $\text{Bi}_3\text{GaMo}_2\text{O}_{12}$ is fitted with Debye expression [25] below 5 K.

$$C_{ph}(T) = 9R \sum c_n \left(\frac{T}{\theta_{Dn}} \right)^3 \int \frac{x^4 e^{-x}}{(e^x - 1)^2} dx$$

Here, the θ_{Dn} represent the Debye temperatures, c_n indicate the multiplication coefficients, and R is the universal gas constant. The extracted Debye temperatures are $\theta_{D1} \approx 240$ K and $\theta_{D2} \approx 308$ K. The fit is extrapolated down to 0.2 K, and then subtracted from the C_p data of $\text{Bi}_3\text{FeMo}_2\text{O}_{12}$. As shown in the inset of Fig. 4, the $C_m(T)$ data show a broad maximum at 6 K, like at 10 K in the $\chi(T)$ data. The appearance of a broad maximum in the C_p data is due to the short-range spin correlations that arise from the one-dimensional nature of exchange interaction between Fe^{3+} moments [6, 18]. It has been noticed in many LDMS that the broad maximum in the heat capacity is generally at low temperatures than that of the broad maximum in susceptibility [6, 26]. The magnetic entropy S_m is calculated from the integration of C_m/T versus T . The estimated entropy S_m increases and saturates to the maximum value of about 14.83 J/mol K ($= R \ln 6$), expected for an $S = 5/2$ system.

The inset of Fig. 5 shows the plot of C_m/T versus T^2 . We have compared the data with the linear and exponential curves. The data do not follow the exponential behavior, ruling out the existence of a spin-gap in the ground state. A very small upturn in C_m/T versus T^2 plot indicates that the system might be reaching a static magnetic long-range ordered state at extremely low temperatures. In Fig. 5, The C_m/T is nearly independent of T at low temperatures ($T \ll J/k_B$), indicating that data follows nearly linear behavior expected for the systems with gapless excitations. From the C_m/T versus T^2 plot, the intercept value is found to be $\gamma \approx 250$ mJ/mol-K². It is somewhat larger than that of $S = 5/2$ linear chain system tetramethyl ammonium manganese trichloride (TMMC) with $J/k_B = -6.7$ K ($\gamma \approx 9.8$ mJ/mol-K²) [27]. From the normalized magnetic heat capacity ($C_m J/Nk_B^2$) [6], the scaled γ value (i.e. $\gamma J/Nk_B^2$) for $\text{Bi}_3\text{FeMo}_2\text{O}_{12}$ ($S = 5/2$ triangular chain) is different from TMMC ($S = 5/2$ linear chain). The results suggest that $S = 5/2$ triangular spin chain system $\text{Bi}_3\text{FeMo}_2\text{O}_{12}$ hosts the robust gapless excitations.

E. DFT calculations

To shed light on the electronic structures and to understand the magnetic behavior of $\text{Bi}_3\text{FeMo}_2\text{O}_{12}$, spin-polarized DFT calculations in the local-spin density approximation (LSDA) and LSDA+ U (Hubbard U) approach were carried out by means of a full-potential linearized muffin-tin orbital (FP-LMTO) method [28, 29] as implemented in the RSPt code [30]. We have considered on-site Coulomb interaction $U = 2$ eV combined with Hund's exchange $J_H = 0.8$ eV within the fully rotationally invariant LSDA+ U approach [31] to treat the electronic correlation effects of Fe- d states. Such choices of U are guided by a previous report on a correlated oxide containing high-spin Fe^{3+} ions [32]. From both LSDA and LSDA+ U calculations, the lowest energy state is identified for the pattern with the antiferromagnetic couplings between the 1st NN and 2nd NN Fe-spins in the isolated zig-zag-chain.

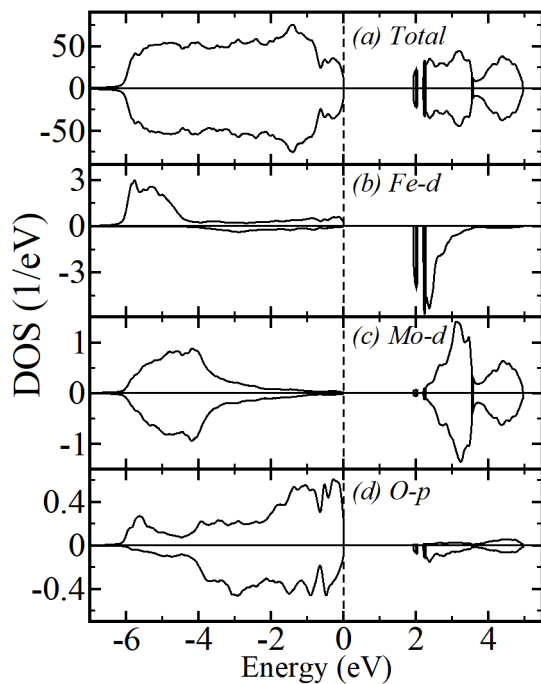


Figure 6: Total and orbital-decomposed density of states (DOS) for the lowest energy magnetic state. Fermi energy is set to zero.

Table I: The details of exchange coupling strengths using LSDA approach with U

	J_1	J_2
Fe-Fe distance	3.8Å	5.3Å
Exchange path	Fe-O1-O1-Fe (Fe-O1-O1=128.5° & O1-O1-Fe=71.9°)	Fe-O2-O2-Fe (Fe-O2-O2=111.8° & O2-O2-Fe=111.8°)
LSDA+ U	-1.52 K	-1.66 K

The computed total and orbital-decomposed density of states (DOS) in this lowest-energy magnetic state as obtained from LSDA+ U are shown in Fig 6(a). The DOS of Fe-3d clearly shows that the majority spin states are fully filled up, and the minority spin states are empty (see Fig.6(b)). This is consistent with the picture of the high-spin ground state of Fe³⁺ ions ($3d^5$). The Mo- d states (see Fig. 6(c)) are found to be completely empty, indicating the nominal d^0 non-magnetic state of these ions. The O- p states are also delocalized and spread in the entire valence band. The insulating gap of 1.7 eV is found between O- p and the Fe- d states, making this system a member of the charge-transfer insulator in the Zaanen, Sawatzky, and Allen (ZSA) scheme [33, 34].

We next estimated the various magnetic exchange couplings (J_1 and J_2 as marked in Fig. 1) based on the converged lowest energy magnetic state. Here we employed the formalism of Ref. [35], where the total converged energies of the magnetic system are mapped onto

a Heisenberg Hamiltonian, and magnetic force theorem [36, 37] is applied to extract the inter-atomic magnetic exchange interactions. Our calculations, as summarized in table I, reveal that both J_1 and J_2 are antiferromagnetic. The J_1 and J_2 exchange interactions are mediated through Fe-O-O-Fe super-exchange paths with varied Fe-Fe distances (3.79 Å and 5.25 Å), as mentioned in table I. Interestingly, the magnitudes of both the exchanges come out to be almost equal ($J_2/J_1 \approx 1.1$) although the corresponding Fe-Fe distances are very different. We also note that such a conclusion is very robust and independent of the adopted methods and independent of U choice within the LSDA+ U approach.

The highly delocalized nature of O- p orbitals promotes such super-super exchange interaction. Interestingly, the Fe-O-O angles that connect the two 2nd NN Fe are equal while these angles are different for 1st NN. The peculiar character of the crystal symmetry is responsible for the reason of having J_1 and J_2 to be nearly equal, despite having a difference in the Fe-Fe bond distances. The nature of the exchange could also be qualitatively understood within the framework of the extended Kugel-Khomskii model [38, 39]. It is well established that half-filled orbitals promote antiferromagnetic super-exchange since virtual hopping between Fe orbitals is allowed only if they possess anti-parallel alignments. Importantly, the antiferromagnetic nature, together with the comparable exchange interactions ($J_1 \approx J_2$), causes strong spin-frustration in the zig-zag-shaped triangular Fe³⁺ chains. The estimated $\theta_{CW} \approx -37.5$ K agrees very well with the experimental value of -40 K, providing further credence to the theoretically computed values of the exchange interactions. The ratio of the inter- to intra-chain magnetic exchange coupling J'/J_1 is estimated at about 0.01. Thus, we can conclude that the present system is an example of a nearly isolated $S = 5/2$ triangular spin chain.

IV. DISCUSSION

Triangular antiferromagnets offer a promising ground for realizing the unusual states of matter. In $S = 5/2$ triangular systems, a few 2D magnets were investigated AFeO₂ (A=Cu, Li, and Na) [40, 41]; however, the quantum ground state without magnetic LRO has not been identified. Achieving the disordered quantum state in $S = 5/2$ systems probably requires a material with ideal one-dimensionality. Our experimental observations on $S = 5/2$ triangular chain material Bi₃FeMo₂O₁₂ ($J_2/J_1 \approx 1.1$ and $J'/J \approx 0.01$) revealed that it exhibits large magnetic frustration ($f > 200$). Besides, the observation of the linear behavior of $C_m(T)$ suggests the presence of gapless excitations. Strikingly, the physics of $S = 5/2$ triangular chain behavior is entirely different from that of the $S = 1/2$ triangular chain, where one can expect a robust spin-gap ground state [16]. As an example, $S = 1/2$ zig-zag chain system Sr_{0.9}Ca_{0.1}CuO₂ has shown the spin-gap ground state due to the randomness

[42]. All the results support that the titled compound might be a possible candidate for gapless spin liquid. Muon spin relaxation and inelastic neutron scattering experiments in sub-Kelvin temperature may shed microscopic insights into the ground state and spin dynamics of the titled material.

V. CONCLUSION

Our investigation reveals that the titled compound $\text{Bi}_3\text{FeMo}_2\text{O}_{12}$ is a nearly ideal quasi-one-dimensional $S = 5/2$ triangular chain system with a small anisotropy ($J_2/J_1 \approx 1.1$). The presence of strong magnetic frustration and negligible inter-chain interactions preclude magnetic LRO down to 200 mK. $C_m(T)$ data show a linear

behavior reflecting the gapless excitations in the ground state. These results will stimulate both theoretical and experimental interests to examine whether our $S = 5/2$ triangular chain $\text{Bi}_3\text{FeMo}_2\text{O}_{12}$ can host the spin liquid ground state.

Acknowledgments: B. K thanks DST INSPIRE faculty award-2014 scheme. We thank Prof. P. L. Paulose and Dr. R. Kumar for their support in magnetic measurements. AKM thanks IIT Tirupati and DST-SERB (Grant No.: ECR/2017/001903), Govt. of India, for providing research grants. The work at SNU were supported by NRF(2019RIA2C2090648 and 2019M3E4A1080227). PK acknowledges the funding by the Science and Engineering Research Board, and Department of Science and Technology, India through Research Grants.

-
- [1] A. N. Vasiliev, O. Volkova, E. Zvereva, and M. Markina, Milestones of low-D quantum magnetism, *Npj Quantum Mater.* **3**, 1 (2018).
- [2] A. N. Vasiliev, O. S. Volkova, E. A. Zvereva, and M. M. Markina, *Low-Dimensional Magnetism*, CRC Press-1st ed., Hardcover Book (2019).
- [3] L. Balents, Spin liquids in frustrated magnets, *Nature* **464**, 199 (2010).
- [4] C. Broholm, R. J. Cava, S. A. Kivelson, D. G. Nocera, M. R. Norman, and T. Senthil, Quantum spin liquids, *Science* **367**, 6475 (2020).
- [5] N. D. Mermin and H. Wagner, Absence of Ferromagnetism or Antiferromagnetism in One or Two-Dimensional Isotropic Heisenberg Models, *Phys. Rev. Lett.* **17**, 1133 (1966).
- [6] D. C. Johnston, R. K. Kremer, M. Troyer, X. Wang, A. Klümper, S. L. Budko, A. F. Panchula, and P. C. Canfield, Thermodynamics of spin $S = 1/2$ antiferromagnetic uniform and alternating-exchange Heisenberg chains, *Phys. Rev. B* **61**, 9558 (2000).
- [7] J. Schlappa, K. Wohlfeld, K. J. Zhou, M. Mourigal, M. W. Haverkort, V. N. Strocov, L. Hozoi, C. Monney, S. Nishimoto, S. Singh, and A. Revcolevschi, Spin-orbital separation in the quasi-one-dimensional Mott insulator Sr_2CuO_3 , *Nature* **485**, 82 (2012).
- [8] M. Mourigal, M. Enderle, A. Klöpperpieper, J. S. Caux, A. Stunault, and H. W. Rønnow, Fractional spinon excitations in the quantum Heisenberg antiferromagnetic chain, *Nature Physics* **9**, 435 (2013).
- [9] C. K. Majumdar, and D. K. Ghosh, On next-nearest-neighbor interaction in linear chain. II, *J. Math. Phys.* **10**, 1399 (1969).
- [10] S. Lebernegg, O. Janson, I. Rousochatzakis, S. Nishimoto, H. Rosner, and A. A. Tsirlin, Frustrated spin chain physics near the Majumdar-Ghosh point in szenic-site $\text{Cu}_3(\text{MoO}_4)(\text{OH})_4$, *Phys. Rev. B* **95**, 035145 (2017).
- [11] A. K. Bera, B. Lake, W. D. Stein, and S. Zander, Magnetic correlations of the quasi-one-dimensional half-integer spin-chain antiferromagnets $\text{SrM}_2\text{V}_2\text{O}_8$ ($M = \text{Co}, \text{Mn}$), *Phys. Rev. B* **89**, 094402 (2014).
- [12] L. D. Sanjeewa, V. O. Garlea, M. A. McGuire, C. D. McMillen, H. B. Cao, and J. W. Kolis, Structural and Magnetic Characterization of the One-dimensional $S = 5/2$ Antiferromagnetic Chain System $\text{SrMn}(\text{VO}_4)(\text{OH})$, *Phys. Rev. B* **93**, 224407 (2016).
- [13] L. D. Sanjeewa, A. S. Sefat, M. Smart, M. A. McGuire, C. D. McMillen, J. W. Kolis, Synthesis, structure and magnetic properties of $\text{Ba}_3\text{M}_2\text{Ge}_4\text{O}_{14}$ ($M = \text{Mn}$ and Fe): Quasi-one-dimensional zig-zag chain compounds, *Journal of Solid State Chemistry* **283**, 121090 (2020).
- [14] P. S. Berdonosov, E. S. Kuznetsova, V. A. Dolgikh, A. V. Sobolev, I. A. Presniakov, A. V. Olenev, B. Rahaman, T. Saha-Dasgupta, K. V. Zakharov, E. A. Zvereva, O. S. Volkova, and A. N. Vasiliev, Crystal structure, physical properties, and electronic and magnetic structure of the spin $S = 5/2$ zig-zag chain compound $\text{Bi}_2\text{Fe}(\text{SeO}_3)_2\text{OCl}_3$, *Inorganic Chemistry* **53**, 5830 (2014).
- [15] A. W. Sleight, and W. Jeitschko, $\text{Bi}_3(\text{FeO}_4)(\text{MoO}_4)_2$ and $\text{Bi}_3(\text{GaO}_4)(\text{MoO}_4)_2$ - new compounds with scheelite related structures, *Materials Research Bulletin* **9**, 951 (1974).
- [16] K. Uematsu, T. Hikihara, and H. Kawamura, Frustration-induced quantum spin liquid behavior in the $S = 1/2$ random-bond Heisenberg antiferromagnet on the zig-zag chain, *arXiv preprint arXiv:2009.08630* (2020).
- [17] C. Li, Z. Gao, X. Tian, J. Zhang, D. Ju, Q. Wu, W. Lu, Y. Sun, D. Cui, and X. Tao, Bulk crystal growth and characterization of the bismuth ferrite-based material $\text{Bi}_3\text{FeO}_4(\text{MoO}_4)_2$, *Cryst Eng Comm*, **21**, 2508 (2019).
- [18] R. Nath, A. V. Mahajan, N. Büttgen, C. Kegler, A. Loidl, and J. Bobroff, Study of one-dimensional nature of $S = 1/2$ (Sr, Ba) $_2\text{Cu}(\text{PO}_4)_2$ and BaCuP_2O_7 via ^{31}P NMR, *Phys. Rev. B* **71**, 174436 (2005).
- [19] B. Koteswararao, R. Kumar, P. Khuntia, Sayantika Bhowal, S. K. Panda, M. R. Rahman, A. V. Mahajan, I. Dasgupta, M. Baenitz, Kee Hoon Kim, and F. C. Chou, Magnetic properties and heat capacity of the three-dimensional frustrated $S = 1/2$ antiferromagnet $\text{PbCuTe}_2\text{O}_6$, *Phys. Rev. B* **90**, 035141 (2014).
- [20] Y. Okamoto, M. Nohara, H. Aruga-Katori, and H. Takagi, Spin-Liquid State in the $S = 1/2$ Hyperkagome Antiferromagnet $\text{Na}_4\text{Ir}_3\text{O}_8$, *Phys. Rev. Lett.* **99**, 137207

- (2007).
- [21] M. E. Fisher, and J. C. Bonner, Linear Magnetic Chains with Anisotropic coupling, *Phys. Rev.* **135**, A640 (1964).
- [22] M. E. Fisher, Magnetism in one-dimensional systems-the Heisenberg model for infinite spin, *American Journal of Physics* **32**, 343 (1964).
- [23] L. J. De Jongh, and A. R. Miedema, Experiments on simple magnetic model systems, *Advances in Physics* **50**, 947 (2001).
- [24] To match both the C_p data at high temperatures from 200 K to 250 K, the C_p data of $\text{Bi}_3\text{GaMo}_2\text{O}_{12}$ is multiplied with 1.09 and then used it for subtracting the lattice of $\text{Bi}_3\text{FeMo}_2\text{O}_{12}$.
- [25] C. Kittel, *Introduction to Solid State Physics*, John Wiley and Sons press - 8th ed., New York, NY (2004).
- [26] B. Koteswararao, S. K. Panda, R. Kumar, Kyongjun Yoo, A. V. Mahajan, I. Dasgupta, B. H. Chen, Kee Hoon Kim, and F. C. Chou, Observation of $S = 1/2$ quasi-1D magnetic and magneto-dielectric behavior in a cubic $\text{SrCuTe}_2\text{O}_6$, *J. Phys. Condens. Matter* **27**, 426001 (2015).
- [27] W. J. M. de Jonge, C. H. W. Swüste, K. Kopinga, and K. Takeda, Specific heat of nearly-one-dimensional tetramethyl ammonium manganese trichloride (TMMC) and tetramethyl ammonium cadmium trichloride (TMCC), *Phys. Rev. B* **12**, 5858 (1975).
- [28] O. K. Andersen, Linear methods in band theory, *Phys. Rev. B* **12**, 3060 (1975).
- [29] J. M. Wills and B. R. Cooper, Synthesis of band and model Hamiltonian theory for hybridizing cerium systems, *Phys. Rev. B* **36**, 3809 (1987).
- [30] J. M. Wills, O. Eriksson, M. Alouni, and D. L. Price, *Electronic Structure and Physical Properties of Solids: The Uses of the LMTO Method* (Springer, Berlin, 2000).
- [31] V. I. Anisimov, I. V. Solovyev, M. A. Korotin, M. T. Czyzyk, and G. A. Sawatzky, Density-functional theory and NiO photoemission spectra, *Phys. Rev. B* **48**, 16929 (1993).
- [32] J. Chakraborty and I. Dasgupta, First principles study of electronic structure, magnetism and ferroelectric properties of rhombohedral AgFeO_2 , *J. Magn. Magn. Mater.* **487**, 165296 (2019).
- [33] J. Zaanen, G. A. Sawatzky and J. W. Allen, Band gaps and electronic structure of transition metal compounds, *Phys. Rev. Lett.* **55**, 418 (1985).
- [34] S. Nimkar, D. D. Sarma, H. R. Krishnamurthy, and S. Ramasesha, Mean-field results of the multiple-band extended Hubbard model for the square-planar CuO_2 lattice, *Phys. Rev. B* **48**, 7355 (1993).
- [35] Y. O. Kvashnin, O. Granas, I. Di Marco, M. I. Katsnelson, A. I. Lichtenstein, and O. Eriksson, Exchange parameters of strongly correlated materials: Extraction from spin-polarized density functional theory plus dynamical mean-field theory, *Phys. Rev. B* **91**, 125133 (2015).
- [36] A. Liechtenstein, M. Katsnelson, V. Antropov, and V. Gubanov, Local spin density functional approach to the theory of exchange interactions in ferromagnetic metals and alloys, *J. Magn. Magn. Mater.* **67**, 65 (1987).
- [37] M. I. Katsnelson and A. I. Lichtenstein, First-principles calculations of magnetic interactions in correlated systems, *Phys. Rev. B* **61**, 8906 (2000).
- [38] K. I. Kugel and D. I. Khomskii, Crystal-structure and magnetic properties of substances with orbital degeneracy, *Zh. Eksp. Teor. Fiz.* **64**, 1429 (1973).
- [39] K. I. Kugel and D. I. Khomskii, The Jahn-Teller effect and magnetism: transition metal compounds, *Sov. Phys. Uspekhi* **25**, 231 (1982).
- [40] F. Ye, Y. Ren, Q. Huang, J. A. Fernandez-Baca, Pengcheng Dai, J. W. Lynn, and T. Kimura, Spontaneous spin-lattice coupling in the geometrically frustrated triangular lattice antiferromagnet CuFeO_2 , *Phys. Rev. B* **73**, 220404(R) (2006).
- [41] M. Tabuchi, K. Ado, H. Sakaebe, C. Masquelier, H. Kageyama, and O. Nakamura, Preparation of AFeO_2 (A= Li, Na) by hydrothermal method, *Solid State Ionics* **79**, 220 (1995).
- [42] F. Hammerath, S. Nishimoto, H.-J. Grafe, A. U. B. Wolter, V. Kataev, P. Ribeiro, C. Hess, S.-L. Drechsler, and B. Büchner, Spin Gap in the zig zag Spin-1/2 Chain Cuprate $\text{Sr}_{0.9}\text{Ca}_{0.1}\text{CuO}_2$, *Phys. Rev. Lett.* **107**, 017203 (2011).